

# 13

## Effect of an intermediate layer on the formation and properties of nanostructured ITO films

© L.K. Markov, I.P. Smirnova, A.S. Pavluchenko, M.A. Yagovkina, A.V. Nashchekin

Ioffe Institute, St. Petersburg, Russia  
E-mail: l.markov@mail.ioffe.ru

Received May 19, 2025

Revised July 8, 2025

Accepted July 17, 2025

The process of growing nanostructured films by magnetron sputtering on glass substrates with and without pre-deposited dense indium-tin oxide (ITO) layers has been studied. It has been shown that the intermediate ITO layer helps the nucleation of nanowires at low temperatures at the initial stages of film growth. Optical measurements have demonstrated antireflection ability of the nanocrystal layer. Taking into account the reduced surface resistance of the obtained films, the proposed method is promising for a wide range of applications, including manufacturing transparent electrodes for optoelectronic devices.

**Keywords:** transparent conductive oxides, indium tin oxide, ITO, nanostructured coatings.

DOI: 10.61011/TPL.2025.10.62124.20376

Indium tin oxide (ITO) is one of the key functional materials in modern optoelectronics due to its unique combination of high electrical conductivity and visible-range optical transparency. The fact that ITO is widely used as transparent conductive contacts for various devices, such as liquid crystal displays, touch panels, LEDs and solar cells, has stimulated active research into ways to control its structural and electrical properties. In recent years, special attention has been paid to nanostructured forms of ITO layers, including porous and nanowire-based ones, which exhibit improved characteristics because of an increase in their specific surface area and realization of new physical effects. New horizons are opening up in applying the material for omnidirectional antireflective coatings with a gradient of the effective refractive index [1], gas sensors [2], medical electrochemical sensors [3], ionic microsupercapacitors [4], in photocatalytic processes [5], electrochromic coatings [6], light-scattering surfaces promoting light coupling from high-refractivity media [7], and field emitters [8].

ITO films containing nanowires (NWs) may be obtained by various methods: pulsed laser deposition [9], molecular beam epitaxy [10], chemical vapor deposition [11], electron beam evaporation [12], ion-assisted electron beam evaporation [1], magnetron sputtering [13]. The NW ITO formation from In–Sn seed droplets proceeds autocatalytically via the vapor-liquid-crystal (VLC) mechanism. Accordingly, this process requires heating the substrate to temperatures exceeding the melting point of the seed droplet metal composition. In [14], we have examined how the substrate temperature affects the morphology of indium tin oxide films deposited on glass substrates by magnetron sputtering. The magnetron sputtering method has a number of advantages over other methods for producing films containing ITO NWs, namely, relative simplicity, virtually unlimited scalability, and, hence, possibility of commercial use.

Here we propose a method for fabricating nanostructured ITO films, which is able to make significantly easier the process of NW nucleation and formation and, hence, allows conducting the process at lower temperatures.

The films were deposited by magnetron sputtering of a high-purity ITO target (99.99 %, 90 %wt. of  $\text{In}_2\text{O}_3$ +10 %wt. of  $\text{SnO}_2$ ) at the direct current of 200 mA ( $P \sim 130$  W) and high-purity (99.999%) argon pressure of 0.3 Pa by using a combined film-deposition setup produced by Torr Int. (USA). As the substrates, borosilicate glass slides 1.2 mm thick were used. Jointly with them, we loaded in the chamber similar substrates pre-coated with smooth dense ITO layers prepared via the commercially available technique on the Astra-S magnetron sputtering setup (Izovac Ltd. (Belarus)). The layer thickness was 170 nm, its surface resistance was  $10 \Omega/\square$ . Fig. 1 presents a scanning electron

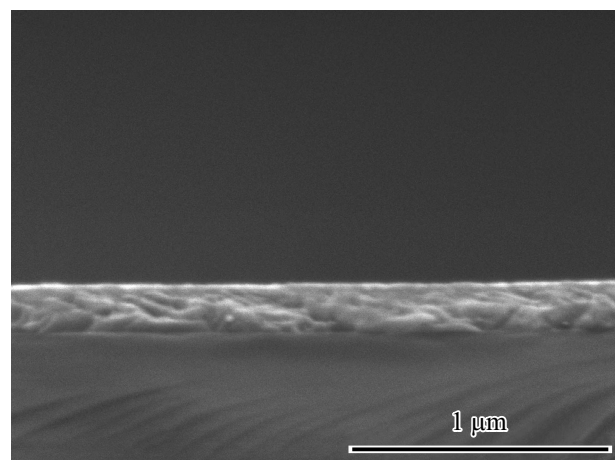


**Figure 1.** SEM image of the initial substrate pre-coated with an ITO layer.

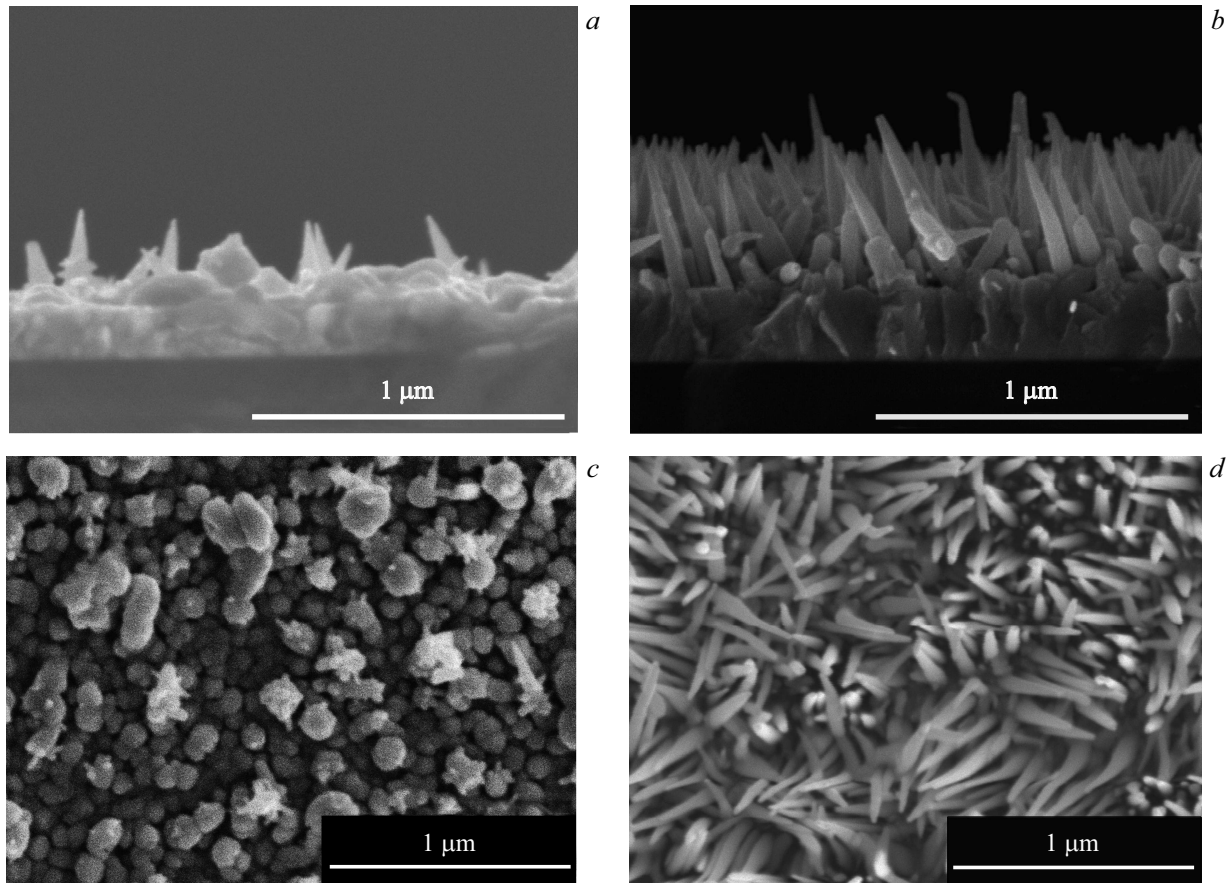


**Figure 2.** SEM images of the cleavage (*a, b*) and top view (*c, d*) of the film deposited at 300 °C on the glass substrate (*a, c*) and on the glass substrate with a dense ITO layer (*b, d*).

microscopy (SEM) image of the ITO-layer-coated substrate used in the experiments. In the experiments, SEM images of the films were obtained with scanning electron microscope JEOL JSM-7001F (JEOL Ltd., Japan).

The substrate temperatures during depositing the nanostructured film was 300 °C, while the mass content of the film substance matched its mass content in an unstructured dense film 150 nm thick. The films were deposited on the substrates in the argon atmosphere. After being deposited, the films were heated to 550 °C and annealed in nitrogen at the same temperature for 10 min without removal from the vacuum chamber. Additional annealing helps to achieve the optimal combination of the films' conductivity and transparency. The transmission and reflection spectra of the samples were studied using spectroradiometer Optronic Laboratories OL 770. The radiation was incident on the sample from the side of the film perpendicular to its surface. X-ray diffraction measurements were performed on diffractometer D2 Phaser Powder (Bruker AXS, Germany). In the experiments, the  $\text{CuK}_{\alpha 1, \alpha 2}$  radiation was used, which was detected by a semiconductor linear position-sensitive detector LYNXEYE (Bruker AXS, Germany) with the opening of 5°. The diffraction curves were interpreted based on the ICDD diffraction database PDF-2, release 2014

(Powder Diffraction File-2, ICDD, 2014), by using special software package EVA (Bruker AXS, Germany).

The SEM data (Fig. 2) shows that the morphology of ITO films obtained in the experiment is determined by the substrate on which the films have been deposited. For instance, at the very beginning of the NW formation during deposition on a pure glass substrate they have small lengths and low surface density (Fig. 2, *a*, and *c*), while in the case of deposition on the substrate pre-coated with a smooth ITO layer pronounced nanowires with a high surface density are formed (Fig. 2, *b* and *d*).

Since initiation of the VLC process needs formation of molten-metal droplets on the substrate surface, the observed effect is associated with a higher probability of droplet formation on the ITO layer surface as compared with that on the glass surface. Probably, at the initial stage of deposition the decisive role is played by the surface wettability by the molten-metal droplets, which in the simplest case is defined by the Young equation for contact wetting angle

$$\cos \theta = \frac{\gamma_{SV} - \gamma_{SL}}{\gamma_{LV}}, \quad (1)$$

where  $\gamma_{SL}$ ,  $\gamma_{SV}$ ,  $\gamma_{LV}$  are the surface tensions at the solid–liquid, solid–vapor and liquid–vapor interfaces, respectively. Hence, an increase in component  $\gamma_{SV}$  will lead

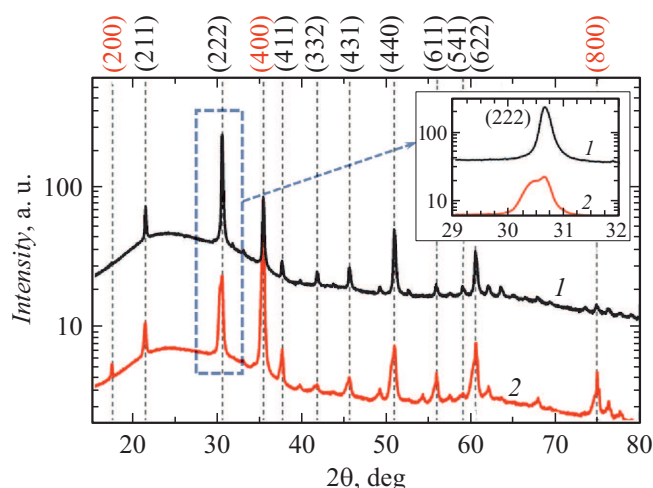


**Figure 3.** Diffraction curves from the sample on pure glass (1) and from that on glass with the ITO sublayer (2). The colored figure is given in the electronic version of the article.

to a decrease in the contact angle. Apparently, surface tension at the glass–vapor interface is significantly higher than that at the ITO–vapor interface, which prevents the droplet formation on the glass surface and promotes creation of a continuous ITO layer. Further, formation of the continuous sublayer on the glass surface is accompanied by variations in the wettability conditions, and droplet formation on the substrate becomes energetically more favorable. Thus, the pre-formed ITO sublayer promotes an earlier and more active growth of NWs. This assumption is consistent with the demonstrated in [15,16] dependences of the density and size distribution of the In–Sn droplets arising on the substrate at the early stage of the ITO film deposition on two factors: substrate surface energy and surface diffusion energy.

X-ray diffraction analysis showed that ITO has a cubic lattice with space group  $Ia-3$ . The presented diffraction patterns (Fig. 3) show clearly that the sample grown on the ITO sublayer has a pronounced texture over planes ( $h00$ ), i.e. NWs stretch in directions perpendicular to the cube face. In the figure, indices of these reflections

are highlighted in red (the color version of the figure is presented in the electronic version of the article). In the curve measured for the ITO sample grown on pure glass, the texture is pronounced only slightly. The diffraction peaks on the curve of the sample grown on the ITO sublayer have a pronounced asymmetry towards smaller angles on the  $2\theta$  scale (see the inset to Fig. 3). This evidences that the sample contains two ITO phases significantly differing in the cell parameters and crystallite sizes.

The results of the diffraction curves profile analysis are listed in the Table. According to the Table data, the NW layer created on the ITO sublayer (row 3 in the Table) is characterized by a larger crystallite size and lower microdeformations, which is associated with specific features of their growth via the VLC mechanism.

Transmission and reflection spectra of the samples under study are given in Fig. 4. The same figure presents the spectra of glass with a smooth ITO film, which was used in the experiment as one of the substrates. As per Fig. 4, both obtained samples have similar optical characteristics allowing using them as contacts for highly efficient optoelectronic devices. Note that, in almost the entire wavelength range, the sample with developed NWs grown on the substrate with an even ITO layer exceeds the substrate itself in transmittance, despite the almost twofold increase in the film specific mass, and, hence, in the light absorption in it. Thus, the nanostructured layer has an antireflective effect on the smooth film due to the presence of gradient of the effective refractive index. The fact that transmittance of the sample with the nanostructured film without the ITO sublayer is higher than that of the film on the ITO sublayer is explainable by that in the first case the film specific mass is lower. The NW layer grown on the ITO sublayer is more efficient in view of light coupling than that grown on glass; this is confirmed by a lower integrated reflectivity of this sample (curve 3 in Fig. 4).

Measurements of the electrical characteristics of the films obtained in the experiment gave the following values of surface resistance:  $29 \Omega/\square$  for the film without the ITO sublayer,  $9 \Omega/\square$  for the film with the ITO sublayer.

Results of the profile analysis of diffraction curves from the studied samples

Sample type	Cell parameter $a$ , Å	Crystallite size, nm	Microdeformation $\varepsilon_0$	Divergence factor of the model and experimental curves $R_{wp}$
NWs on the pure glass substrate	10.159	200	$8.4 \cdot 10^{-4}$	2.2
NWs on the glass substrate with the ITO layer	10.196	60	$17.7 \cdot 10^{-4}$	4.2
	10.139	300	$7.0 \cdot 10^{-4}$	

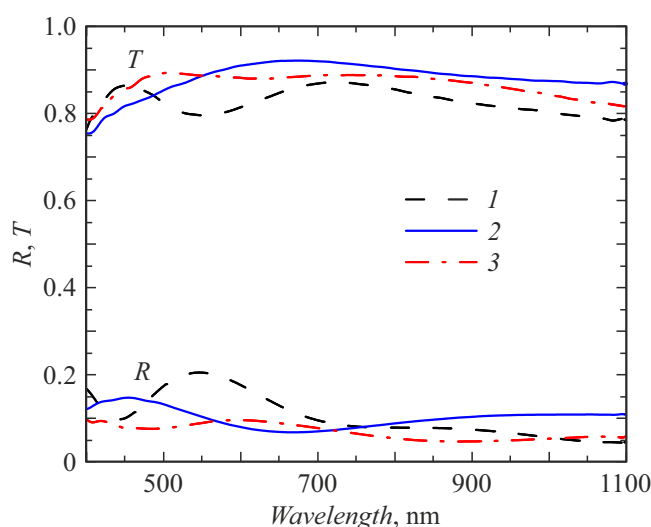


**Figure 4.** Transmission and reflection spectra of samples with different coatings: initial substrate with the smooth ITO layer (1), nanostructured ITO layer deposited on pure glass (2), and glass with the smooth ITO sublayer (3).

As mentioned above, the ITO sublayer surface resistance was  $10 \Omega/\square$ .

Thus, in this paper we propose a new method for creating nanostructured ITO films, which involves preliminary deposition of a dense even ITO sublayer onto the glass substrate. As a result, the process of the ITO NW formation is significantly simplified due to variations in the substrate surface wettability by the In–Sn droplets. Concurrent reduction in the surface electrical resistance of the nanostructured samples allows using these films in applications requiring high current densities. The gradient of the effective refractive index caused by the ITO layer nanostructure has an antireflective effect, that is, it increases the film transmittance and reduces its reflection.

## Acknowledgements

X-ray diffraction measurements and SEM investigation were performed by using facilities of the Federal CCU „Materials Science and Diagnostics in Advanced Technologies“ (Ioffe Institute).

## Conflict of interests

The authors declare that they have no conflict of interests.

## References

- [1] T. Chaikereee, N. Mungkung, N. Kasayapanand, H. Nakajima, T. Lertvanithphol, K. Tantiwanichapan, A. Sathukarn, M. Horprathum, *Opt. Mater.*, **129**, 112439 (2022). DOI: 10.1016/J.OPTMAT.2022.112439
- [2] X. Zheng, X. Qiao, F. Luo, B. Wan, C. Zhang, *Sens. Actuators B*, **346**, 130440 (2021). DOI: 10.1016/J.SNB.2021.130440
- [3] J. Suo, K.X. Jiao, J.H. Yi, D. Fang, O. Ruzimuradov, *J. Cent. South Univ.*, **31** (3), 747 (2024). DOI: 10.1007/s11771-024-5590-y
- [4] Y. Ding, Y. Lin, Y. Zhang, H. Jiang, M. Su, E. Xie, Z. Zhang, *Appl. Phys. Lett.*, **125** (6), 063902 (2024). DOI: 10.1063/5.0220141
- [5] J. Suo, K. Jiao, D. Fang, H. Bu, Y. Liu, F. Li, O. Ruzimuradov, *Vacuum*, **204**, 111338 (2022). DOI: 10.1016/J.VACUUM.2022.111338
- [6] L. Filatov, V. Chernyavsky, I. Ezhov, L. Markov, A. Pavluchenko, I. Smirnova, P. Vishniakov, N. Yurchenko, P. Zhukov, M. Maximov, *Mater. Today Commun.*, **44**, 112116 (2025). DOI: 10.1016/J.MTCOMM.2025.112116
- [7] A.S. Pavluchenko, L.K. Markov, I.P. Smirnova, V.V. Aksenova, M.V. Mesh, D.S. Kolokolov, *Mater. Lett.*, **372**, 137040 (2024). DOI: 10.1016/J.MATLET.2024.137040
- [8] Z. An, Y. Shen, X. Xu, F. Shi, F. Song, Y. Yu, J. Dong, Y. Xu, L. Zhang, J. Zhao, *J. Nanopart. Res.*, **26** (6), 132 (2024). DOI: 10.1007/s11051-024-06044-w
- [9] G. Meng, T. Yanagida, K. Nagashima, H. Yoshida, M. Kanai, A. Klamchuen, F. Zhuge, Y. He, S. Rahong, X. Fang, S. Takeda, T. Kawai, *J. Am. Chem. Soc.*, **135** (18), 7033 (2013). DOI: 10.1021/ja401926u
- [10] C. O'Dwyer, M. Szachowicz, G. Visimberga, V. Lavayen, S.B. Newcomb, C.M.S. Torres, *Nat. Nanotechnol.*, **4** (4), 239 (2009). DOI: 10.1038/nnano.2008.418
- [11] S.M. Yang, H.K. Yen, K.C. Lu, *Nanomaterials*, **12** (6), 897 (2022). DOI: 10.3390/nano12060897
- [12] Y. Shen, Y. Zhao, J. Shen, X. Xu, *JOM*, **69** (7), 1155 (2017). DOI: 10.1007/s11837-017-2353-3
- [13] Y. Zhang, Q. Li, Z. Tian, P. Hu, X. Qin, F. Yun, *SN Appl. Sci.*, **2** (2), 264 (2020). DOI: 10.1007/s42452-020-2050-7
- [14] L.K. Markov, A.S. Pavluchenko, I.P. Smirnova, V.V. Aksenova, M.A. Yagovkina, V.A. Klinkov, *Thin Solid Films*, **774**, 139848 (2023). DOI: 10.1016/J.TSF.2023.139848
- [15] H.K. Yu, J.L. Lee, *Sci. Rep.*, **4** (1), 6589 (2014). DOI: 10.1038/srep06589
- [16] H.K. Yu, W.J. Dong, G.H. Jung, J.L. Lee, *ACS Nano*, **5** (10), 8026 (2011). DOI: 10.1021/nn2025836

*Translated by EgoTranslating*